# Theory for transport through a single magnetic molecule: Endohedral N@$C_{60}$

Florian Elste* and Carsten Timm†
*Institut für Theoretische Physik, Freie Universität Berlin, Arnimallee 14, D-14195 Berlin, Germany*
(Received 28 October 2004; revised manuscript received 21 December 2004; published 7 April 2005)

We consider transport through a single N@$C_{60}$ molecule, weakly coupled to metallic leads. Employing a density-matrix formalism we derive rate equations for the occupation probabilities of many-particle states of the molecule. We calculate the current-voltage characteristics and the differential conductance for N@$C_{60}$ in a break junction. Our results reveal Coulomb-blockade behavior as well as a fine structure of the Coulomb-blockade peaks due to the exchange coupling of the $C_{60}$ spin to the spin of the encapsulated nitrogen atom.

DOI: 10.1103/PhysRevB.71.155403 PACS number(s): 85.65.+h, 75.50.Xx

## I. INTRODUCTION

The rapid progress of miniaturization of electronic devices has led to chip features smaller than 100 nm, for which standard semiconductor technology reaches its limit. One proposed solution is a transistor consisting of a single molecule. In recent years transport through single molecules has been studied quite extensively[1–6]—for example, in break junctions.[7–9] *Inelastic* transport occurs due to the interaction of electrons with internal vibrational or magnetic degrees of freedom of the molecules. Transport through magnetic molecules[10–12] is particularly interesting also from the point of view of *spintronics*—i.e., the idea of exploiting the electron spin in electronic devices. While most molecules are normally nonmagnetic, there are exceptions such as endohedral N@$C_{60}$—i.e., a nitrogen atom encapsulated in a $C_{60}$ cage.[13] It is known that the encapsulated atom retains its $p$ electrons,[13] leading to a localized spin $S_N=3/2$. There are fascinating ideas of employing this spin in a quantum computer.[14]

In this paper we propose to measure the current through a single N@$C_{60}$ molecule in a break junction and we calculate the current-voltage ($I$-$V$) characteristics and the differential conductance $dI/dV$. Since transport through a single $C_{60}$ molecule has been demonstrated[8] and the synthesis of endohedral fullerenes is also feasible,[13] such an experiment is possible with present-day apparatus. Besides the typical Coulomb-blockade behavior we predict a characteristic fine structure of the Coulomb-blockade peaks in $dI/dV$ due to the exchange coupling of the $C_{60}$ spin to the spin $3/2$ of the encapsulated nitrogen atom. It should be mentioned that the discussion of transport through P@$C_{60}$ proceeds quite analogously and yields qualitatively identical results.

## II. THEORY

In our model the N@$C_{60}$ molecule is treated as a quantum dot and the leads, labeled as L (left) and R (right), as macroscopic charge reservoirs. Relaxation in the leads is assumed to be sufficiently fast so that the electron distributions in the leads can be described by Fermi functions. As $C_{60}$ generally prefers to be singly or doubly negatively charged,[15–19] we assume that electronic transport through the molecule involves only the threefold-degenerate LUMO (lowest unoccupied molecular orbital).[20] Since we concentrate on the fine structure of the differential conductance close to degeneracy points, we assume that the fivefold-degenerate HOMO (highest occupied molecular orbital), which lies about 7.5 eV below the LUMO,[18] remains fully occupied, whereas the threefold-degenerate LUMO+1, about 1.7 eV above the LUMO,[18] remains empty.[21] Charge transfer from the nitrogen atom to the fullerene cage is assumed to be negligible. When the LUMO is partially occupied, the net spin of the electrons in the LUMO, $\mathbf{S}_{C_{60}}$, couples to the spin $3/2$ of the nitrogen atom, $\mathbf{S}_N$, and the total spin of the molecule is $\mathbf{S}=\mathbf{S}_{C_{60}}+\mathbf{S}_N$. The exchange interaction can be written in the simple form $-J\mathbf{S}_{C_{60}}\cdot\mathbf{S}_N$ due to Hund's first rule: Note that the three LUMO's and the three nitrogen $p$ orbitals both have odd parity with a single nodal plane each, which can be chosen as the $xy$, $yz$, or $zx$ plane. Consequently, there is only a significant exchange interaction between any LUMO and the $p$ orbital of the same symmetry. The exchange interaction can thus be written as a sum of terms for the three pairs of orbitals. However, due to the strong Hund's-rule coupling, the $p$-orbital spins combine to $S_N=3/2$; i.e., they are all parallel. Then the spin of each $p$ orbital is $\mathbf{S}_N/3$, as can be proved by projecting the spins onto the $S_N=3/2$ subspace. Thus the exchange terms can be combined to the simple scalar product. The full Hamiltonian of the system then reads $H=H_d+H_{leads}+H_t$, where

$$H_d=(\varepsilon-eV_g)n_d+\frac{U}{2}n_d(n_d-1)-J\mathbf{S}_{C_{60}}\cdot\mathbf{S}_N \tag{1}$$

represents the molecular quantum dot,

$$H_{leads}=\sum_{\alpha=L,R}\sum_{\mathbf{k}\sigma}\epsilon_{\alpha\mathbf{k}}a^\dagger_{\alpha\mathbf{k}\sigma}a_{\alpha\mathbf{k}\sigma} \tag{2}$$

represents the leads, and

$$H_t=\sum_{\alpha=L,R}\sum_{n\mathbf{k}\sigma}(t_\alpha a^\dagger_{\alpha\mathbf{k}\sigma}c_{n\sigma}+t^*_\alpha c^\dagger_{n\sigma}a_{\alpha\mathbf{k}\sigma}) \tag{3}$$

describes the tunneling between dot and leads, which is assumed to be weak compared to typical excitation energies of the molecule. Here, the operator $c^\dagger_{n\sigma}$ creates an electron with spin $\sigma$ in the molecular orbital $n$, while $a^\dagger_{\alpha\mathbf{k}\sigma}$ creates an electron in lead $\alpha$ with spin $\sigma$, momentum $\mathbf{k}$, and energy $\epsilon_{\alpha\mathbf{k}}$ relative to the Fermi energy. $n_d=\Sigma_{n\sigma}c^\dagger_{n\sigma}c_{n\sigma}$ and

 

$\mathbf{S}_{C_{60}}=\Sigma_{n\sigma\sigma'}c^{\dagger}_{n\sigma}(\boldsymbol{\sigma}_{\sigma\sigma'}/2)c_{n\sigma'}$ are the number and spin operators of electrons on the dot, respectively. Electron-electron interaction is taken into account by the local Coulomb repulsion $U$ and the exchange interaction with the nitrogen spin by the exchange coupling $J$. The values of $\varepsilon$, $U$, and $J$ are not well known at present. *Ab initio* calculations[16–18] indicate that $C_{60}^{-}$ is the ground state, whereas $C_{60}^{2-}$ has a slightly higher energy. This is in agreement with the experimental observation of a very-long-lived metastable $C_{60}^{2-}$ (Ref. 15). However, there are recent contradicting *ab initio* results predicting $C_{60}^{2-}$ to be slightly bound relative to $C_{60}^{-}$ (Ref. 19). For our numerical calculations we use $\varepsilon=-2.75$ eV and $U=2.84$ eV in accordance with Ref. 17. $J$ appears to be *ferromagnetic*. We take $J\sim 1$ meV from the *ab initio* calculations of Udvardi.[22] This relatively strong exchange coupling is consistent with the absence of electron-paramagnetic-resonance (EPR) signals for $N@C_{60}$ anions with charges $-1$ through $-5$, while the signal is present for the neutral molecule and the hexa-anion.[23] Note that the exchange coupling is significantly smaller than the energy of relevant vibrational modes. The oscillations of the molecule as a whole have an energy of the order of 5 meV.[8] The oscillations of the nitrogen atom within the $C_{60}$ have an energy of 13 meV,[24] whereas the modes of the $C_{60}$ cage lie at much higher energies.

We next derive rate equations for this model starting from the equation of motion for the density matrix $\rho$,[5,6,25] $d\rho_I(t)/dt=-i[H_{tI},\rho_I(t)]$. Here, the index $I$ denotes the interaction representation with respect to $H_t$. Integration and iteration gives[5,25]

$$\frac{d\rho_I(t)}{dt}=-i[H_{tI}(t),\rho_I(0)]-\int_0^t dt'[H_{tI}(t),[H_{tI}(t'),\rho_I(t')]]. \tag{4}$$

Assuming that the leads are weakly affected by the quantum dot and neglecting correlations between the two, $\rho_I(t)$ can be replaced by the direct product of the *reduced density matrix* of the dot, $\rho_{dI}(t)\equiv \mathrm{Tr}_{\mathrm{leads}}\,\rho_I(t)$, and the density matrix $\rho_{\mathrm{leads}}$ of the leads, $\rho_I(t)\approx\rho_{dI}(t)\otimes\rho_{\mathrm{leads}}$. We then obtain

$$\frac{d\rho_{dI}(t)}{dt}=-\int_0^t dt'\ \mathrm{Tr}_{\mathrm{leads}}[H_{tI}(t),[H_{tI}(t'),\rho_{dI}(t')\otimes\rho_{\mathrm{leads}}]]. \tag{5}$$

Returning to the Schrödinger representation and using the Markov approximation[5,25] $\rho_{dI}(t')\approx\rho_{dI}(t)$, we find

$$\frac{d\rho_d(t)}{dt}=-i[H_d,\rho_d]-\mathrm{Tr}_{\mathrm{leads}}\int_0^\infty dt'[H_t,[e^{-i(H_d+H_{\mathrm{leads}})t'}\times H_t e^{i(H_d+H_{\mathrm{leads}})t'},\rho_d(t)\otimes\rho_{\mathrm{leads}}]] \tag{6}$$

as the equation of motion for $\rho_d$. This expression shows that the tunneling Hamiltonian $H_t$ is treated in second-order perturbation theory. Taking the trace over the degrees of freedom of the leads produces Fermi functions according to

$$\mathrm{Tr}_{\mathrm{leads}}\,\rho_{\mathrm{leads}}a^{\dagger}_{\alpha\mathbf{k}\sigma}a_{\alpha'\mathbf{k}'\sigma'}=\delta_{\alpha\alpha'}\delta_{\mathbf{k}\mathbf{k}'}\delta_{\sigma\sigma'}f(\epsilon_{\alpha\mathbf{k}}-\mu_\alpha), \tag{7}$$

where $\mu_\alpha$ denotes the chemical potential of lead $\alpha$ due to the applied source-drain voltage $V$. Expanding the nested commutators in Eq. (6) and inserting Eq. (3) gives eight terms:

$$\begin{aligned}\frac{d\rho_d(t)}{dt}=-\int_0^\infty dt'\sum_{\alpha nn'\mathbf{k}\sigma}|t_\alpha|^2\{&f(\epsilon_{\alpha\mathbf{k}}-\mu_\alpha)e^{i\epsilon_{\alpha\mathbf{k}}t'}c_{n\sigma}e^{-iH_dt'}c^{\dagger}_{n'\sigma}e^{iH_dt'}\rho_d(t)+[1-f(\epsilon_{\alpha\mathbf{k}}-\mu_\alpha)]e^{-i\epsilon_{\alpha\mathbf{k}}t'}c^{\dagger}_{n\sigma}e^{-iH_dt'}c_{n'\sigma}e^{iH_dt'}\rho_d(t)\\&-[1-f(\epsilon_{\alpha\mathbf{k}}-\mu_\alpha)]e^{i\epsilon_{\alpha\mathbf{k}}t'}c_{n\sigma}\rho_d(t)e^{-iH_dt'}c^{\dagger}_{n'\sigma}e^{iH_dt'}-f(\epsilon_{\alpha\mathbf{k}}-\mu_\alpha)e^{-i\epsilon_{\alpha\mathbf{k}}t'}c^{\dagger}_{n\sigma}\rho_d(t)e^{-iH_dt'}c_{n'\sigma}e^{iH_dt'}\\&-[1-f(\epsilon_{\alpha\mathbf{k}}-\mu_\alpha)]e^{-i\epsilon_{\alpha\mathbf{k}}t'}e^{-iH_dt'}c_{n\sigma}e^{iH_dt'}\rho_d(t)c^{\dagger}_{n'\sigma}-f(\epsilon_{\alpha\mathbf{k}}-\mu_\alpha)e^{i\epsilon_{\alpha\mathbf{k}}t'}e^{-iH_dt'}c^{\dagger}_{n\sigma}e^{iH_dt'}\rho_d(t)c_{n'\sigma}\\&+f(\epsilon_{\alpha\mathbf{k}}-\mu_\alpha)e^{-i\epsilon_{\alpha\mathbf{k}}t'}\rho_d(t)e^{-iH_dt'}c_{n\sigma}e^{iH_dt'}c^{\dagger}_{n'\sigma}+[1-f(\epsilon_{\alpha\mathbf{k}}-\mu_\alpha)]e^{i\epsilon_{\alpha\mathbf{k}}t'}\rho_d(t)e^{-iH_dt'}c^{\dagger}_{n\sigma}e^{iH_dt'}c_{n'\sigma}\}.\end{aligned} \tag{8}$$

The probability of the dot being in the many-particle state $|n\rangle$ is $P^n\equiv\langle n|\rho_d(t)|n\rangle$. Introducing the overlap matrix elements $C^{\sigma}_{mn}\equiv\langle m|\Sigma_i c_{i\sigma}|n\rangle$ and $C^{\sigma\dagger}_{mn}\equiv\langle m|\Sigma_i c^{\dagger}_{i\sigma}|n\rangle$ and identifying the integrals in Eq. (8) as $\delta$ functions we can write Eq. (8) as a set of rate equations

$$\frac{dP^n}{dt}=\sum_{m\neq n}P^mR_{m\to n}-P^n\sum_{m\neq n}R_{n\to m}, \tag{9}$$

with transition rates

$$R_{n\to m}=\sum_{\alpha\sigma}2\pi|t_\alpha|^2D_\alpha f(\epsilon^d_m-\epsilon^d_n-\mu_\alpha)(|C^{\sigma}_{nm}|^2+|C^{\sigma}_{mn}|^2). \tag{10}$$

Here, $\epsilon^d_n$ is the energy of the many-particle state $|n\rangle$ of the dot and $D_\alpha$ denotes the density of states per spin species in lead $\alpha$, which we take to be constant and equal for both leads. The matrix elements $C^{\sigma}_{mn}$ ($C^{\sigma\dagger}_{mn}$) can only be finite if the electron number of state $|n\rangle$ is larger (smaller) by 1 than the electron number of state $|m\rangle$. We are interested in the *stationary state*, which corresponds to $dP^n/dt=0$ for all states $|n\rangle$.

In deriving Eq. (9) we have assumed that the density ma-

trix $\rho_d$ is *completely diagonal*. This assumption requires some thought since many of the eigenstates of our molecular quantum dot are degenerate so that one might expect finite off-diagonal components even in the stationary state. However, this is not the case: Let $U$ be a unitary matrix that leaves the dot Hamiltonian $H_d$ invariant. With any stationary density matrix $\rho_d$, $U\rho_d U^\dagger$ is another solution. Now suppose that there exists a stationary solution $\rho_d$ that is *not* diagonal within a block of degenerate states. Then one can choose $U$ so that $U\rho_d U^\dagger$ is diagonal since the nonzero off-diagonal components have been assumed to connect degenerate states (we exclude the case of accidental degeneracy). But then $U\rho_d U^\dagger$ has *unequal* diagonal components—i.e., probabilities $P^n$—for symmetry-related states. This is clearly unphysical. On the other hand, if $\rho_d$ is already diagonal with degenerate dot states having equal diagonal components, any allowed transformation $U$ leaves $\rho_d$ invariant.

The current operator for lead $\alpha = \mathrm{L,R}$ reads[26]

$$I_\alpha = i[H, N_\alpha] = -i\sum_{n\mathbf{k}\sigma} (t_\alpha c^\dagger_{n\sigma} a_{\alpha\mathbf{k}\sigma} - t^*_\alpha a^\dagger_{\alpha\mathbf{k}\sigma} c_{n\sigma}), \qquad (11)$$

where $N_\alpha$ is the number operator for electrons in lead $\alpha$. Tracing out the leads we arrive at an expression for the expectation value of the current:

$$\langle I_\alpha \rangle = 2\pi D_\alpha |t_\alpha|^2 \sum_{ml\sigma} (f(\epsilon^d_l - \epsilon^d_m - \mu_\alpha)|C^\sigma_{ml}|^2 - [1 - f(\epsilon^d_m - \epsilon^d_l - \mu_\alpha)]|C^\sigma_{lm}|^2) P^m. \qquad (12)$$

We here consider the symmetric case $t_L = t_R$ and $\mu_L = -\mu_R = V/2$.

As there are $\binom{6}{i}$ possible ways of filling the threefold-degenerate $C_{60}$ LUMO with $i$ electrons according to the Pauli principle and as the nitrogen atom possesses a spin $3/2$, solving the rate equations and calculating the current reduces to an eigenvalue problem of dimension $4\Sigma_{i=0}^{6}\binom{6}{i} = 256$.

### III. RESULTS AND DISCUSSION

The $I$-$V$ characteristics plotted in Fig. 1 show a conductance gap for $|V| < 0.18$ V due to the Coulomb blockade. Our numerical results show that the current $I$ is symmetric with respect to the applied source-drain voltage $V$ in accordance with the high symmetry of the fullerene molecule. Each step in the main $I$-$V$ curve corresponds to the opening of additional current channels. Simultaneously, the average occupation $\langle n \rangle$ of the dot changes. For the parameters chosen above, the $C_{60}^-$ state is the ground state.[17] At the first step, the potential drop becomes large enough to allow transitions between the nearly degenerate charge states −1 and −2, as the chemical potential $\mu_L = V/2$ reaches the value assumed for the ionization energy $E(C_{60}^{2-}) - E(C_{60}^-) = \varepsilon + U = 0.09$ eV. At the second step, transitions between the charge states −1 and 0 become possible, etc.

Our results for the occupation probabilities reveal that detailed balance is satisfied for the broad plateaus in Fig. 1—i.e., $P^n R_{n\to m} = P^m R_{m\to n}$. As a consequence, the dot occupation probabilities $P^n$ for all *occupied* states are identical in the limit $T \to 0$, as the transition rates $R_{n\to m}$ are symmetric

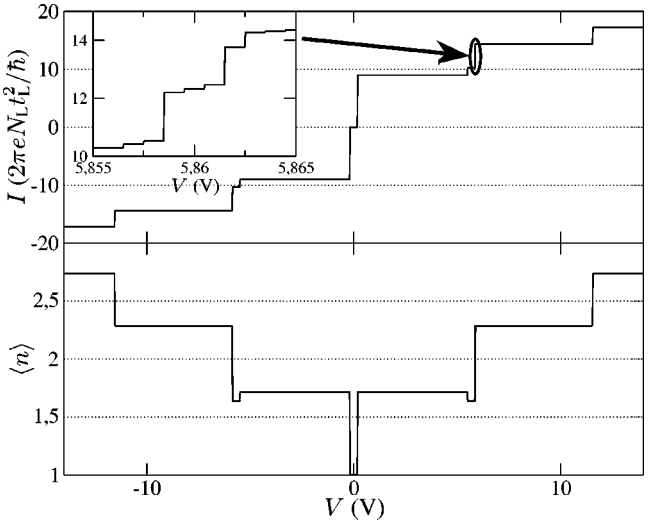


FIG. 1. Current $I$ and average occupation $\langle n \rangle$ of the $C_{60}$ LUMO as a function of the source-drain voltage $V \equiv \mu_L - \mu_R$ for $\varepsilon = -2.75$ eV, $U = 2.84$ eV, $J = 1$ meV, $V_g = 0$ V, and $T = 0.01$ K. The inset shows the fine structure of one particular Coulomb-blockade step.

for each pair $n,m$ of occupied states. This also accounts for the fact that the average occupation $\langle n \rangle$ is exactly unity for $V = 0$ V, increases to $(24\times 1 + 60\times 2)/(24+60) = 12/7 \approx 1.71$ at the first step, when the molecule is in one of 24 singly charged or 60 doubly charged states with equal probability, and decreases to $(4\times 0 + 24\times 1 + 60\times 2)/(4+24+60) = 18/11 \approx 1.64$ at the second step, when 4 additional neutral states become available, etc. Furthermore, we find that each Coulomb-blockade step shows a characteristic fine structure, which we discuss below.

The calculation of the differential conductance $dI/dV$ as a function of source-drain voltage $V$ and gate voltage $V_g$ shows the usual *Coulomb diamonds*; see Fig. 2. Close to the degeneracy points between different charge states we observe a relatively complex fine structure, corresponding to the steps in the inset of Fig. 1. We assume very low temperatures, $k_B T \ll J$, to exhibit the structure more clearly. At higher temperatures the peaks in $dI/dV$ are thermally broadened. In the following, we briefly explain the physics behind the fine structure, taking Fig. 2(a) as an example.

Since the $C_{60}$ spin $S_{C_{60}}$, the spin of the nitrogen atom, $S_N$, and the total spin $S$ (where $S = |S_{C_{60}} - S_N|, \ldots, S_{C_{60}} + S_N$) are good quantum numbers, the exchange energy is

$$E_{\mathrm{exc}} = -\frac{J}{2}[S(S+1) - S_{C_{60}}(S_{C_{60}}+1) - S_N(S_N+1)], \qquad (13)$$

which leads to the level splitting illustrated in Fig. 3. The structure in Fig. 2(a) arises from transitions between charge states −1 and −2, taking spin excitations into account. In equilibrium ($V = 0$ V) only the ground state of the dot is occupied, which is the $C_{60}^-$ state with $S_{C_{60}} = 1/2$ and $S = 2$ for $V_g$ smaller than the degeneracy point $V_g^0$ and the $C_{60}^{2-}$ state with $S_{C_{60}} = 1$ and $S = 5/2$ for $V_g > V_g^0$; cf. Fig. 3(a). For $V_g < V_g^0$ the *first* peak in $dI/dV$ at nonzero $V$ originates from

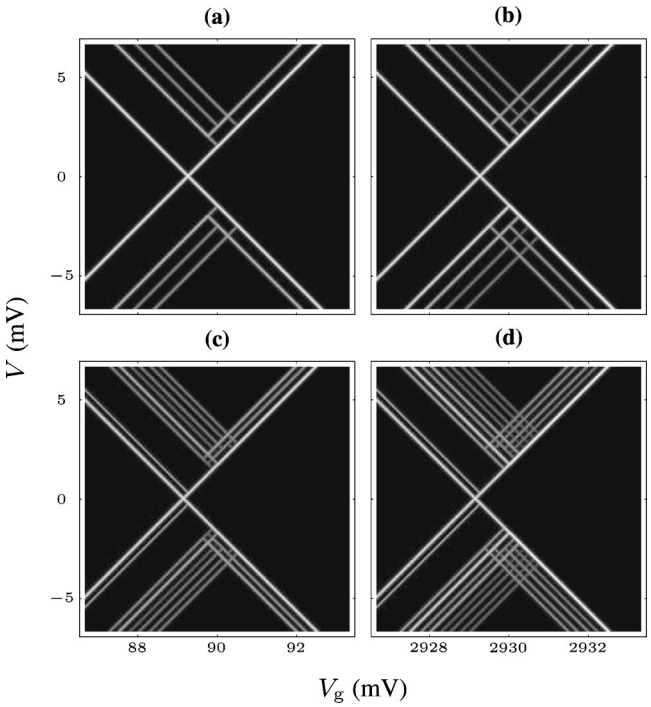


FIG. 2. Gray-scale plots of the differential conductance $dI/dV$ as a function of source-drain voltage $V$ and gate voltage $V_g$ for $T=0.1$ K. Shown are two particular ranges of gate voltages close to the degeneracy points between charge states −1 and −2 (a),(c) and between −2 and −3 (b),(d). (a) and (b) show results for vanishing magnetic field and (c) and (d) for $B=2$ T.

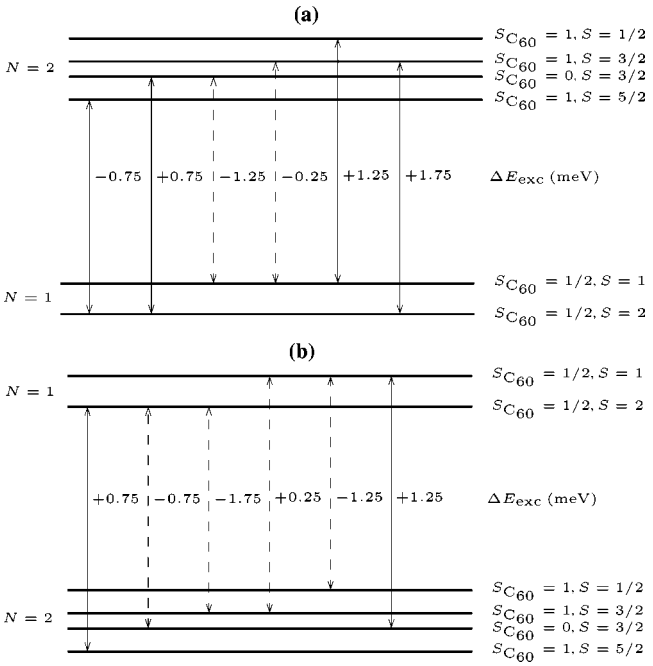


FIG. 3. Energy levels and all allowed transitions between many-particle states with one ($N=1$) and two ($N=2$) electrons, taking into account spin excitations. (a) Situation with the $N=1$ multiplet lower in energy than the $N=2$ multiplet. (b) Reverse case.

the transition with $S_{C_{60}}=1/2\rightarrow 1$ and $S=2\rightarrow 5/2$, corresponding to a gain of exchange energy of $\Delta E_{exc}=-0.75$ meV. The *second* peak results from a transition with $S_{C_{60}}=1/2\rightarrow 0$, $S=2\rightarrow 3/2$, and $\Delta E_{exc}=+0.75$ meV. Simultaneously, the transitions with $S_{C_{60}}=1/2\rightarrow 0$, $S=1\rightarrow 3/2$, and $\Delta E_{exc}=-1.25$ meV and $S_{C_{60}}=1/2\rightarrow 1$, $S=1\rightarrow 3/2$, and $\Delta E_{exc}=-0.25$ meV are enabled [dashed lines in Fig. 3(a)]. Although energetically possible, these transitions are not excited at lower source-drain voltages, because the lower levels are unoccupied. The last two peaks belong to transitions with $S_{C_{60}}=1/2\rightarrow 1$, $S=1\rightarrow 1/2$, and $\Delta E_{exc}=+1.25$ meV and $S=1/2\rightarrow 1$, $S=2\rightarrow 3/2$, and $\Delta E_{exc}=+1.75$ meV. Note that the values of $\Delta E_{exc}$ account for the level spacing.

The situation is different for $V_g$ significantly larger than $V_g^0$, where we observe only two peaks; cf. Fig. 2(a). As soon as the transition from the $C_{60}^{2-}$ ground state into the lowest $C_{60}^{-}$ state with $S_{C_{60}}=1\rightarrow 1/2$, $S=5/2\rightarrow 2$, and $\Delta E_{exc}=+0.75$ meV becomes possible, the transitions corresponding to $\Delta E_{exc}=-0.75$ meV, −1.75 meV, +0.25 meV, and −1.25 meV [dashed lines in Fig. 3(b)] are also enabled. Again the latter four would be energetically possible at lower $V$, but do not appear as peaks of $dI/dV$, since the corresponding lower levels are unoccupied. In the vicinity of $V_g^0$ we find that the slope of several lines abruptly changes sign. This corresponds to the situation where two levels connected in Fig. 3 by a transition cross as $V_g$ is varied. The fine structure in Fig. 2(b) can be discussed analogously. The structure is different for all degeneracy points and can thus serve as a *fingerprint* of the particular charge transition. This should be useful since the zero of the $V_g$ axis is often shifted significantly from one experiment to the next.

Selection rules for single-electron tunneling require that $\Delta S_{C_{60}}=\pm 1/2$ and $\Delta S=\pm 1/2$. The different brightness of the peaks in Fig. 2 is correlated with the number of transitions that are possible at a given source-drain voltage. Each allowed transition may be thought of as one current channel.

Experimentally, the *magnetic* origin of the fine structure is most conclusively tested by observing the behavior in a magnetic field. For ionized $C_{60}$ in lattices and in solution, the orbital moment is quenched.[27,28] We assume that the fields generated by the electrodes in a break junction are also sufficiently strong to quench the orbital moment. Then the molecule couples to a magnetic induction $B$ only through the *spin* moments, described by the new Hamiltonian

$$H' = H - g\mu_B B S^z_{C_{60}} - g\mu_B B S^z_N = H - g\mu_B B S^z. \qquad (14)$$

Here, $\mu_B$ is the Bohr magneton and $g$ is the $g$ factor, which is $g\approx 2$ for both the nitrogen spin $\mathbf{S}_N$ and the $C_{60}$ spin. We choose a many-particle basis of simultaneous eigenstates of $n_d$, $S_{C_{60}}$, $S$, and $S^z$. Then the only difference is that additional Zeeman energies appear in our expression for the transition rates, Eq. (10). In Figs. 2(c) and 2(d) we show $dI/dV$ for the same parameters as in Figs. 2(a) and 2(b) but with $B=2$ T. As expected, the peaks split, but in addition several peaks are absent since they are not allowed by the selection rules. For example, for $V_g > V_g^0$ the first peak is due to a transition with $S_{C_{60}}=1\rightarrow 1/2$, $S=5/2\rightarrow 2$, and $N=2\rightarrow 1$. Since the initial state has all spins aligned in parallel, one electron tunneling

out of the dot can only reduce $S^z$ so that there is only a *single* peak in $dI/dV$.

To summarize, we have presented a theory for transport through a single $N@C_{60}$ molecule weakly coupled to metallic electrodes. Our results for the differential conductance $dI/dV$ as a function of the source-drain and gate voltages show Coulomb blockade and exhibit a characteristic fine structure of the Coulomb-blockade peaks due to the coupling of the $C_{60}$ spin to the spin of the encapsulated nitrogen atom.

## ACKNOWLEDGMENTS

We would like to thank W. Harneit, J. Koch, A. Mitra, and F. von Oppen for helpful discussions and the Deutsche Forschungsgemeinschaft for support through Sonderforschungsbereich 290.

*Electronic address: felste@physik.fu-berlin.de
†Electronic address: timm@physik.fu-berlin.de

[1] C. Joachim, J. K. Gimzewski, and A. Aviram, Nature (London) **408**, 541 (2000).
[2] E. G. Emberly and G. Kirczenow, Chem. Phys. **281**, 311 (2002); Phys. Rev. Lett. **91**, 188 301 (2003).
[3] A. Nitzan and M. A. Ratner, Science **300**, 1384 (2003).
[4] Y. Xue and M. A. Ratner, Phys. Rev. B **68**, 115 406 (2003); **68**, 115 407 (2003).
[5] A. Mitra, I. Aleiner, and A. J. Millis, Phys. Rev. B **69**, 245 302 (2004).
[6] J. Koch and F. von Oppen, cond-mat/0409667 (unpublished).
[7] M. A. Reed, C. Zhou, C. J. Muller, T. P. Burgin, and J. M. Tour, Science **278**, 252 (1997).
[8] H. Park, J. Park, A. K. L. Lim, E. H. Anderson, A. P. Alivisatos, and P. L. McEuen, Nature (London) **407**, 57 (2000).
[9] H. B. Weber, J. Reichert, F. Weigend, R. Ochs, D. Beckmann, M. Mayor, R. Ahlrichs, and H. v. Löhneysen, Chem. Phys. **281**, 113 (2002); J. Reichert, H. B. Weber, M. Mayor, and H. v. Löhneysen, Appl. Phys. Lett. **82**, 4137 (2003).
[10] J. Park, A. N. Pasupathy, J. I. Goldsmith, C. Chang, Y. Yaish, J. R. Petta, M. Rinkoski, J. P. Sethna, H. D. Abruña, P. L. McEuen, and D. C. Ralph, Nature (London) **417**, 722 (2002).
[11] W. Liang, M. P. Shores, M. Bockrath, J. R. Long, and H. Park, Nature (London) **417**, 725 (2002).
[12] C. Durkan and M. E. Welland, Appl. Phys. Lett. **80**, 458 (2002).
[13] T. Almeida Murphy, T. Pawlik, A. Weidinger, M. Höhne, R. Alcala, and J.-M. Spaeth, Phys. Rev. Lett. **77**, 1075 (1996).
[14] W. Harneit, Phys. Rev. A **65**, 032 322 (2002).
[15] R. L. Hettich, R. N. Compton, and R. H. Ritchie, Phys. Rev. Lett. **67**, 1242 (1991).
[16] M. R. Pederson and A. A. Quong, Phys. Rev. B **46**, 13 584 (1992).
[17] C. Yannouleas and U. Landman, Chem. Phys. Lett. **217**, 175 (1994).
[18] M. Wierzbowska, M. Lüders, and E. Tosatti, J. Phys. B **37**, 2685 (2004).
[19] J. Luo, L.-M. Peng, Z. Q. Xue, and J. L. Wu, J. Chem. Phys. **120**, 7998 (2004).
[20] N. Laouini, O. K. Andersen, and O. Gunnarsson, Phys. Rev. B **51**, 17 446 (1995).
[21] Since the LUMO+1 has even parity, whereas the nitrogen *p* orbitals are odd, the exchange interaction with the LUMO+1 is negligible.
[22] L. Udvardi, in *The Exchange Coupling Between the N Atom and the Fullerene Cage in* $N@C_{60}$, in Electronic Properties of Novel Materials—Molecular Nanostructures, edited by H. Kuzmany *et al.*, AIP Conf. Proc. No. 544 (AIP, Melville, NY, 2000), p. 187.
[23] P. Jakes, B. Goedde, M. Waiblinger, N. Weiden, K.-P. Dinse, and A. Weidinger, in *Synthesis and EPR Studies of* $N@C_{60}$ *and* $N@C_{70}$ *Radical Anions*, in Electronic Properties of Novel Materials—Molecular Nanostructures, edited by H. Kuzmany, J. Fink, M. Mehring, and S. Roth, AIP Conf. Proc. No. 544 (AIP, Melville, NY, 2000), p. 174.
[24] F. Uhlík, Z. Slanina, and E. Ōsawa, in *Thermodynamic Properties of* $N@C_{60}$, in Electronic Properties of Novel Materials—Molecular Nanostructures, edited by H. Kuzmany *et al.*, AIP Conf. Proc. No. 544 (AIP, Melville, NY, 2000), p. 183.
[25] K. Blum, *Density Matrix Theory and Applications* (Plenum, New York, 1981).
[26] G. D. Mahan, *Many-particle Physics*, 3rd ed. (Kluwer, New York, 2000).
[27] T. Kato, T. Kodama, M. Oyama, S. Okazaki, T. Shida, T. Nakagawa, Y. Matsui, S. Suzuki, H. Shiromaru, K. Yamauchi, and Y. Achiba, Chem. Phys. Lett. **186**, 35 (1991); T. Kato, T. Kodama, and T. Shida, *ibid.* **205**, 405 (1993).
[28] E. Tosatti, N. Manini, and O. Gunnarsson, Phys. Rev. B **54**, 17 184 (1996), and references therein.